RSC Advances

PAPER

View Article Online
View Journal | View Issue

Check for updates

Cite this: *RSC Adv.*, 2017, **7**, 33373

Insight on lithium polysulfide intermediates in a Li/S battery by density functional theory†

Qi Liu,[a] Daobin Mu,*[a] Borong Wu,*[ab] Lei Wang,[a] Liang Gai[a] and Feng Wu[ab]

Received 26th April 2017
Accepted 20th June 2017

DOI: 10.1039/c7ra04673a

rsc.li/rsc-advances

Soluble lithium polysulfide intermediates dissolve and shuttle during the process of charge/discharge, leading to the rapid capacity decline of a Li–S battery. Density functional theory (DFT) computation is used to research the thermodynamic behavior of the polysulfides. The computation indicates that the stable molecular structures tend to be in a ring shape. This is helpful for cathode modification at a molecular level to fix the polysulfides.

Open Access Article. Published on 03 July 2017. Downloaded on 9/6/2024 5:52:32 AM.
This article is licensed under a Creative Commons Attribution-NonCommercial 3.0 Unported Licence.

With a growing demand from sophisticated functions in portable digital products to application in electric vehicles, a high energy storage system has become a necessity in our daily lives.[1–4] Compared with conventional lithium-ion batteries, the Li–S battery exhibits a higher energy density of 2600 W h kg^{-1}; the cathode of the Li–S battery enjoys a high theoretical specific capacity of 1672 mA h g^{-1},[5,6] which is much higher that of the lithium ion battery, which is generally less than 300 mA h g^{-1}. So, the Li–S battery has attracted more and more attention as a promising next generation energy storage system.[7–13] In addition, the larger resource reserve of sulfur on the earth and the lower cost of sulfur provide strong market competitiveness. However, many challenges are still facing the Li–S battery technology. The first problem is the electrical insulation of sulfur;[14] the second and the main problem for the Li–S battery cathode is the dissolution and shuttle behavior of polysulfide. Soluble lithium polysulfide intermediates (Li_2S_x, $2 < x < 8$) dissolve in organic electrolyte and shuttle from the cathode to the anode, leading to rapid capacity decline and low columbic efficiency.[15,16] The poor electron conductivity of sulfur has been greatly improved by coupling high conductive materials such as multiwalled carbon nanotubes and graphene oxide. The dissolution and shuttle of polysulfides need to be studied further.

As for the dissolution of polysulfides in the Li–S battery, much work has been done to modify the (S) cathode.[12,17–22] Zhang *et al.* have proposed a unique strategy by building a cooperative interface between the S cathode and a separator to suppress the polysulfide shuttle and enhance the reaction kinetics with LDH@NG separators.[23] They also have designed a polar hybrid host material of TiC nanoparticles, which is grown within a porous graphene framework to localize the mobile polysulfide intermediates by chemisorption.[24] In addition, chemical modification using N or O dopants has been proved to significantly enhance the interaction between the carbon hosts and the polysulfide guests, thereby effectively preventing the shuttle of polysulfides.[25] Furthermore, research on electrolytes is also important to understand the mechanism of polysulfide dissolution and reaction.[26] An *in situ* ^{7}Li NMR technique has been used to probe the transient polysulfide redox reactions involving charged free radicals as intermediate species.[27] A cation permselective membrane has been introduced to improve the stability and coulombic efficiency of lithium–sulfur batteries by confining the polysulfides on the cathode side.[28] Different kinds of solvent structures have been investigated by changing the ratio of ether/alkyl moieties to vary the solubility of lithium polysulfide.[29] The chemical reactivity of polysulfides with carbonate-based electrolytes has been investigated, and it is found that the polysulfides react with carbonate-based electrolytes *via* a nucleophilic addition or substitution reaction, leading to a sudden capacity fading of lithium–sulfur cells.[30] First principles calculation has been carried out on the energetic and electronic properties of Li_2S_2, showing that Li_2S_2 is subject to spontaneous disproportionation.[31] Synchrotron high-energy X-ray diffraction analysis and *in situ* transmission electron microscopy have been used to characterize dry powder deposits from lithium polysulfide solution and the lithium diffusion to sulfur.[32] DFT calculations have revealed that Li_2S_8 accepts electrons more readily than S_8 and Li_2S_6, so that it is thermodynamically and kinetically unstable.[33] A solvent-in-salt electrolyte has been used in a Li–S cell, which can inhibit dissolution of polysulfide.[9] The salt decomposition, solvation effects, interactions among

[a]*Beijing Key Laboratory of Environment Science and Engineering, School of Material Science and Engineering, Beijing Institute of Technology, Beijing 100081, China. E-mail: mudb@bit.edu.cn*

[b]*Collaborative Innovation Center of Electric Vehicles in Beijing, Beijing, 100081, China. E-mail: wubr@bit.edu.cn*

† Electronic supplementary information (ESI) available: Distances of all S–S bonds in lithium polysulfides after optimization. The distances and binding energy between polysulfide ions and lithium ions in DOL and DME solvation. Two videos for the process of structure optimization for Li_2S_6 in DOL and DME. The solvation structure of Li_2S_6 in the polarized continuum model of DOL and DME respectively. The curve of Gibbs free energy of Li^+ solvation. The calculated Raman spectroscopy of lithium polysulfides. See DOI: 10.1039/c7ra04673a

Open Access Article. Published on 03 July 2017. Downloaded on 9/6/2024 5:52:32 AM.
This article is licensed under a Creative Commons Attribution-NonCommercial 3.0 Unported Licence.

intermediate products and other species have been investigated by density functional theory and *ab initio* molecular dynamics simulations.[34] The theoretical predictions and experimental observations have also confirmed that DOL prefers to react with Li metal and release C_2H_4 gas, while the DME molecule has good stability.[35] Although research on polysulfides from the point of view of the electrolyte has been given attention, the stable three-dimensional molecular structures of polysulfides in solution are rarely involved. In particular, the three-dimensional molecular structures of polysulfides could provide guidance for the modification of the cathode at a molecular level to fix polysulfides. In addition, the polysulfide degradation mechanism is still controversial, and this is a complex problem. Although some polysulfide mechanisms have been proposed,[36–39] none of them could completely explain the reaction mechanism of the Li–S battery. The reaction contains complicated disproportionation. No single technique is capable of identifying and quantifying the polysulfide species.[40] Fundamental thermodynamics steady state research could also analyze the polysulfide degradation mechanism, and the S–S bond breaking of polysulfides also needs to be further investigated to understand the distribution and transformation of polysulfides and to suppress the shuttle effect by researching the binding energies of S–S bonds. Oleg Borodin *et al.* have researched the solvation in carbonate esters by different kinds of quantum chemistry calculation and simulation.[41–46] Lithium polysulfides in ether solvation should be further researched.

In this work, the DFT method is used to systematically research lithium polysulfide and its possible degradation in the Li–S battery. The stable three-dimensional molecular structure, solvation energy and the dissociation of polysulfides are studied in DOL and DME, respectively. The detailed calculations and analysis will be reported in this work.

Quantum chemical calculations were completed through the density functional theory (DFT) method with Becke's three parameters (B3) exchange functional along with the Lee–Yang–Parr (LYP) nonlocal correlation functional (B3LYP). All the structural optimizations were treated at B3LYP/6-31+G(d,p) level. In order to make zero-point energy (ZPE) corrections, frequency analyses are made with the corresponding basis sets. All the single point energy calculations were performed at B3LYP/6-311++G(3df,3dp) level for more accurate calculation. The outer solvation shells were also considered by using polarized continuum models (PCM). The outer shells solvent effects were completed by geometry optimization at C-PCM-B3LYP/6-31+G(d,p) in DOL solvent (dielectric constant of 7.1) and DME solvent (dielectric constant of 7.2), respectively. In addition, counterpoise corrections were employed to minimize the "Basis Set Superposition Error" (BSSE) when calculating binding energies. All of the DFT calculations were performed with the Gaussian 09 program package.[47]

Ionic association interactions are typically classified as either solvent-separated ion pair (SSIP), contact ion pair (CIP), or aggregate (AGG) coordination, depending upon whether the anions form coordinate bonds with zero, one, or more than one Li^+ cations, respectively.[41–44] In order to study the dissolution and dissociation of the lithium polysulfides, the CIP model is employed to optimize the stable three-dimensional molecular structures of lithium polysulfides in solution (Li_2S_x, $1 \leq x \leq 8$) by the DFT method. Fig. 1 shows the molecular structure of lithium polysulfides (Li_2S_x, $1 \leq x \leq 8$) in DOL. Six DOL molecules around one of the polysulfides are employed to simulate the solvation in all the quantum chemistry optimizations.

Fig. 1(a–f) show the solvated structures of Li_2S, Li_2S_2, Li_2S_3, Li_2S_4, Li_2S_5, Li_2S_6, Li_2S_7 and Li_2S_8 in DOL, respectively. From the figure, it can clearly be seen that the short chain lithium polysulfides (Li_2S_x, $1 \leq x \leq 3$) have a linear sawtooth structure, but for the long chain lithium polysulfides (Li_2S_x, $4 \leq x \leq 8$), the solvated structures tend to be rings. In a previous study, many of the long chain polysulfides were regarded as linear chains. Our calculated results demonstrate that the stable long chain polysulfides have a cyclic structure, which is helpful for recognizing the polysulfides at a molecular level, which could better guide the modification of the cathode to suppress the shuttle of the polysulfides. Video 1† shows the process of structural optimization for Li_2S_6 which is surrounded by six DOL molecules (see ESI Video 1†). It can clearly be seen that at the beginning of the optimization the structure of Li_2S_6 is linear sawtooth, but as the optimization proceeds, the structure of Li_2S_6 gradually shrinks to a cyclic structure. In addition, the outer solvation shells of DOL are also considered by using PCM, and the optimized result also demonstrates that the stable structure of Li_2S_6 is cyclic under solvation conditions, and the implicit solvent has a negligible effect on the structure of lithium polysulfide (see Fig. S1†). LiTFSI is also introduced into the solvation structure, which indicates that the structure of polysulfide is also cyclic with the existence of LiTFSI (see Fig. S2†). The theoretical calculations demonstrate that a cyclic structure for long chain lithium polysulfides (Li_2S_x, $4 \leq x \leq 8$) is more stable in the DOL solvent. In addition, it can clearly be seen that there is no evident interaction between DOL and S_n groups; the DOL combines more easily with a Li atom. Therefore, it should be the case that the polar O atoms in the DOL combine with the Li atom in lithium polysulfides forming complexes in the

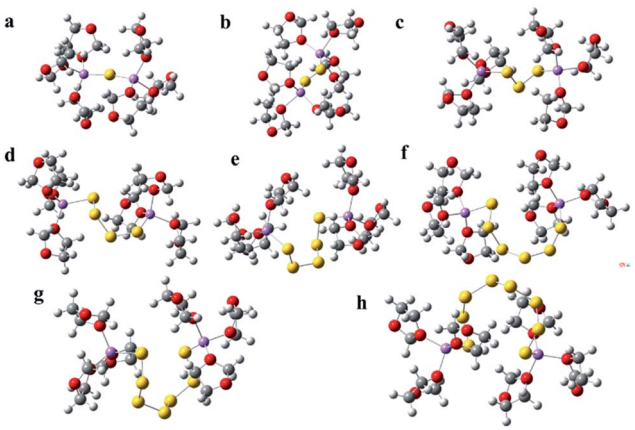

Fig. 1 The solvation structure of lithium polysulfides (Li_2S_x, $1 \leq x \leq 8$, a–h) in DOL solvent; the lithium polysulfide geometries are surrounded by six DOL molecules. Dark gray, white, red, yellow and violet spheres denote C, H, O, S and Li atoms/ions, respectively.

 This journal is © The Royal Society of Chemistry 2017

Open Access Article. Published on 03 July 2017. Downloaded on 9/6/2024 5:52:32 AM.
This article is licensed under a Creative Commons Attribution-NonCommercial 3.0 Unported Licence.

dissolution process. And the Li–S bond is elongated, leading to the stronger negative electricity of the S_n groups, which accelerates the destruction of crystal structure for lithium polysulfides, owing to the two like electric charges of the S_n groups repelling each other. Therefore, the dissolution of lithium polysulfides should be ascribed to the solvation of the Li^+ group when using a DOL solvent. It is also indicated that one Li^+ combines with at most four DOL and three DME by ΔG calculation (see Fig. S3†). The dissolution of lithium polysulfides is in accord with the dissociation of lithium polysulfides.

Furthermore, the solvation of lithium polysulfides in DME was investigated. Four DME molecules are employed to surround the lithium polysulfides. This is similar to the solvation structures in DOL solvent; the short chains of lithium polysulfides (Li_2S_x, $1 \leq x \leq 3$) have a linear sawtooth structure, but the long chains of lithium polysulfides (Li_2S_x, $4 \leq x \leq 8$) have a cyclic structure in DME solvent (see Fig. 2). Video 2† also shows the optimization process of Li_2S_6 in DME solvent (see ESI Video 2†). From the video, it can be clearly seen that the linear sawtooth structure of Li_2S_6 gradually transforms to the ring structure in the optimization process. Fig. S4† also shows the optimized structure of Li_2S_6 in the outer solvation shells of DME by using PCM, and the cyclic structure is clearly shown. Therefore, the calculation results suggest that the cyclic structure for the long chain lithium polysulfides is more stable in both DOL and DME solvents. The difference for the solvation structure of lithium polysulfides in DME is that the lithium ions tend to locate on the middle of the S_n group at both ends, but for the DOL solvent, the lithium ions locate on the respective ends of the S_n group.

Moreover, the binding energies of all S–S bonds in lithium polysulfides in both DOL and DME solvent were analysed after optimization. The binding energies of S–S bonds are calculated by splitting all the lithium polysulfides at every S–S bond. Table 1 exhibits the S–S binding energies in DOL solvent. The binding energies of S^1–S^2, S^2–S^3 and S^3–S^4 for Li_2S_4 are 1.989, 1.465 and 1.986, respectively. The results suggest that the S^2–S^3 may be previously broken to form two S_2. The binding energies of S^1–S^2, S^2–S^3, S^3–S^4 and S^4–S^5 for Li_2S_5 are 2.225, 1.472, 1.36 and 2.304 eV, respectively. This indicates that the S^2–S^3 or S^3–S^4 bonds may break to S_2 and S_3. Perla B. Balbuena[48] *et al.*'s calculation also indicates that S_5 later decomposes into $S_3 + S_2$ and S_3 into $S_2 + S$. In addition, the binding energies of S^1–S^2, S^2–S^3, S^3–S^4, S^4–S^5 and S^5–S^6 bonds for Li_2S_6 are 2.344, 1.487, 1.242, 1.647 and 2.238 eV, indicating that S^3–S^4 might be broken into two S_3. Similarly, the S^3–S^4 bond may undergo bond rupture and form S_3 and S_4 radicals in Li_2S_7. For the Li_2S_8, the S^3–S^4 or S^5–S^6 bond may be broken into S_3 and S_5 radicals.

Table 2 shows the binding energies of S–S bonds in lithium polysulfides after optimization in DME solvent. The binding energy of the S^2–S^3 for the Li_2S_4 is 2.109 eV, which is less than that of the S^1–S^2 (2.435 eV) and S^3–S^4 (2.435 eV), indicating that the two S_2 radicals may be formed more easily. For the Li_2S_5, S_3 and S_2 formation may occur. The binding energy of the S^3–S^4 bond (3.151 eV) is the minimum for Li_2S_6, indicating that two S_3 may be formed by breaking the S^3–S^4 bond. For the Li_2S_7, S_3 and S_4 may be obtained easily. Similarly, for the Li_2S_8, S^3–S^4 (3.441 eV) or S^5–S^6 (3.44 eV) may be broken to S_3 and S_5. *Ab initio* molecular dynamics simulation also suggests that the PS chain

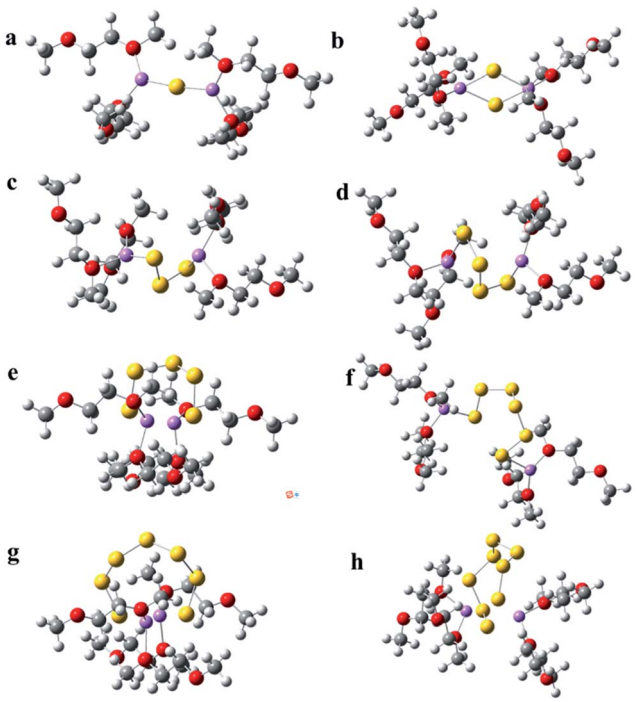

Fig. 2 The solvation structure of polysulfide (Li_2S_x, $1 \leq x \leq 8$, a–h) in DME solvent; the polysulfide geometries are surrounded by four DME molecules. Dark grey, white, red, yellow and violet spheres denote C, H, O, S and Li atoms/ions, respectively.

Table 1 Binding energies of all S–S bonds in polysulfides after optimization in DOL solvent. The energy unit is eV

DOL	S^1–S^2	S^2–S^3	S^3–S^4	S^4–S^5	S^5–S^6	S^6–S^7	S^7–S^8
Li_2S_2	3.319	—	—	—	—	—	—
Li_2S_3	2.018	2.127	—	—	—	—	—
Li_2S_4	1.989	1.465	1.986	—	—	—	—
Li_2S_5	2.225	1.472	1.36	2.304	—	—	—
Li_2S_6	2.344	1.487	1.242	1.647	2.238	—	—
Li_2S_7	2.321	1.663	1.407	1.527	1.62	2.309	—
Li_2S_8	2.37	1.689	1.262	1.829	1.319	1.769	2.303

Table 2 Binding energies of all S–S bonds in polysulfide ions after optimization in DME solvent. The energy unit is eV

DME	S^1–S^2	S^2–S^3	S^3–S^4	S^4–S^5	S^5–S^6	S^6–S^7	S^7–S^8
Li_2S_2	3.561	—	—	—	—	—	—
Li_2S_3	2.861	2.745	—	—	—	—	—
Li_2S_4	2.435	2.109	2.435	—	—	—	—
Li_2S_5	3.914	3.348	2.865	4.103	—	—	—
Li_2S_6	4.079	3.457	3.151	3.457	4.079	—	—
Li_2S_7	3.985	3.609	3.162	3.468	3.415	4.148	—
Li_2S_8	4.135	3.676	3.441	3.817	3.44	3.677	4.135

Open Access Article. Published on 03 July 2017. Downloaded on 9/6/2024 5:52:32 AM.
This article is licensed under a Creative Commons Attribution-NonCommercial 3.0 Unported Licence.

of Li_2S_8 reacts with two Li atoms and, in most cases, it was observed to break into Li_2S_3 and Li_2S_5.[49]

The Raman spectra of lithium polysulfides in a DOL solvation structure were also calculated. Fig. S5† shows the Raman spectra of Li_2S_n ($2 \leq n \leq 8$), which clearly show that polysulfide species generally stay in the wavenumber region of 150–550 cm^{-1}, which is in accord with previous studies.[50–54] In addition, characteristic polysulfide Raman position lines can be found in the area between 400 and 500 cm^{-1} (S–S stretch vibration) and below 250 cm^{-1} (bending and torsional modes).[51]

Conclusions

The lithium polysulfide reaction mechanism is crucial for the high energy density Li–S battery. DFT calculations suggest that the stable molecular structure for short chain lithium polysulfides (Li_2S_x, $1 \leq x \leq 3$) is linear sawtooth, but the stable molecule structure for long chain lithium polysulfides (Li_2S_x, $4 \leq x \leq 8$) tends to a ring in both DOL and DME solvents, which is important for cathode modification at a molecular level to fix the polysulfides. In addition, S_2 and S, two S_2, S_3 and S_2, two S_3, S_3 and S_4, and S_3 and S_5 may be formed by the decomposition of Li_2S_3, Li_2S_4, Li_2S_5, Li_2S_6, Li_2S_7, and Li_2S_8, respectively in both DOL and DME solvation. Furthermore, the mechanism of lithium polysulfide decomposition is complicated, and more combinational work of calculation and experiment is needed to clarify it completely. In addition, further investigations with SSIP and AGG models are needed to understand the solvation of lithium polysulfides.

Acknowledgements

This project was financially supported by NSAF (Grant No. U1530155); the the International Science & Technology Cooperation Program of China under contract No. 2016YFE0102200; the National Key Basic Research Program of China (Contract No. 2015CB251100); Industry University Research Project in Shenzhen (Contract No. 2012CXHZ008).

Notes and references

1 P. Simon and Y. Gogotsi, *Nat. Mater.*, 2008, **7**, 845.
2 P. G. Bruce, B. Scrosati and J.-M. Tarascon, *Angew. Chem., Int. Ed.*, 2008, **47**, 2930.
3 M. Winter and R. J. Brodd, *Chem. Rev.*, 2004, **104**, 4245.
4 B. Kang and G. Ceder, *Nature*, 2009, **458**, 190.
5 S. Evers and L. F. Nazar, *Acc. Chem. Res.*, 2013, **46**, 1135.
6 R. Demir-Cakan, M. Morcrette, F. Nouar, C. Davoisne, T. Devic, D. Gonbeau, *et al.*, *J. Am. Chem. Soc.*, 2011, **133**, 16154.
7 P. G. Bruce, S. A. Freunberger, L. J. Hardwick and J.-M. Tarascon, *Nat. Mater.*, 2012, **11**, 19.
8 X. Ji, K. T. Lee and L. F. Nazar, *Nat. Mater.*, 2009, **8**, 500.
9 L. Suo, Y.-S. Hu, H. Li, *et al.*, *Nat. Commun.*, 2013, **4**.
10 A. Manthiram, Y. Fu and Y.-S. Su, *Acc. Chem. Res.*, 2013, **46**, 1125.
11 A. Manthiram, Y. Fu, S.-H. Chung, C. Zu and Y.-S. Su, *Chem. Rev.*, 2014, **114**, 11751.
12 Z. Li, J. Zhang, *et al.*, *Angew. Chem., Int. Ed.*, 2015, **53**, 12886.
13 X. Gu, S. Zhang and Y. Hou, *Chin. J. Chem.*, 2016, **34**, 13.
14 X.-B. Cheng, H.-J. Peng, J.-Q. Huang, R. Zhang, C.-Z. Zhao and Q. Zhang, *ACS Nano*, 2015, **9**, 6373.
15 M.-K. Song, Y. Zhang and E. J. Cairns, *Nano Lett.*, 2013, **13**, 5891.
16 X. Liang, Z. Wen, Y. Liu, H. Zhang, J. Jin, M. Wu and X. Wu, *J. Power Sources*, 2012, **206**, 409.
17 R. Sahore, L. P. Estevez, A. Ramanujapuram, F. J. DiSalvo and E. P. Giannelis, *J. Power Sources*, 2015, **297**, 188–194.
18 J. Zhang, Y. Cai, Q. Zhong, *et al.*, *Nanoscale*, 2015, **7**, 17791.
19 L. Qie and A. Manthiram, *Adv. Mater.*, 2015, **27**, 1694.
20 R. Fang, S. Zhao, P. Hou, M. Cheng, S. Wang, H. M. Cheng, C. Liu and F. Li, *Adv. Mater.*, 2016, **28**, 3374.
21 M. R. Kaiser, X. Liang, H. K. Liu, S. X. Dou and J. Z. Wang, *Carbon*, 2016, **103**, 163.
22 X. Chen, H. Peng, R. Zhang, T. Hou, J. Huang, B. Li and Q. Zhang, *ACS Energy Lett.*, 2017, **2**, 795.
23 H. Peng, Z. Zhang, J. Huang, G. Zhang, J. Xie, W. Xu, J. Shi, X. Chen, X. Cheng and Q. Zhang, *Adv. Mater.*, 2016, **28**, 9551.
24 H. Peng, G. Zhang, X. Chen, Z. Zhang, W. Xu, J. Huang and Q. Zhang, *Angew. Chem.*, 2016, **128**, 13184.
25 T. Hou, X. Chen, H. Peng, J. Huang, B. Li, Q. Zhang and B. Li, *Small*, 2016, **12**, 3283.
26 K. Xu, *Chem. Rev.*, 2014, **114**, 11503.
27 J. Xiao, J. Z. Hu, H. Chen, M. Vijayakumar, J. Zheng, H. Pan, E. D. Walter, *et al.*, *Nano Lett.*, 2015, **15**, 3309.
28 J.-Q. Huang, Q. Zhang, H.-J. Peng, X.-Y. Liu, W.-Z. Qian and F. Wei, *Energy Environ. Sci.*, 2014, **7**, 347.
29 C. Barchasz, J.-C. Lepretre, S. Patoux and F. Alloin, *Electrochim. Acta*, 2013, **89**, 737.
30 T. Yim, M.-S. Park, J.-S. Yu, K. J. Kim, K. Y. Im, J.-H. Kim, G. Jeong, Y. N. Jo, *et al.*, *Electrochim. Acta*, 2013, **107**, 454.
31 Z. Feng, C. Kim, A. Vijh, M. Armand, K. H. Bevan and K. Zaghib, *J. Power Sources*, 2014, **272**, 518.
32 R. Xu, I. Belharouak, X. Zhang, R. Chamoun, C. Yu, Y. Ren, A. Nie, R. Shahbazian-Yassar, J. Lu, *et al.*, *ACS Appl. Mater. Interfaces*, 2014, **6**, 21938.
33 J.-J. Chen, R.-M. Yuan, J.-M. Feng, Q. Zhang, J.-X. Huang, G. Fu, M.-S. Zheng, *et al.*, *Chem. Mater.*, 2015, **27**, 2048.
34 L. E. Camacho-Forero, T. W. Smith and P. B. Balbuena, *J. Phys. Chem. C*, 2017, **121**, 182–194.
35 X. Chen, T. Hou, B. Li, C. Yan, L. Zhu, C. Guan, X. Cheng, H. Peng, J. Huang, Q. Zhang, DOI: 10.1016/j.ensm.2017.01.003.
36 N. A. Canas, S. Wolf, N. Wagner and K. Friedrich, *J. Power Sources*, 2013, **226**, 313.
37 M. Cuisinier, P.-E. Cabelguen, S. Evers, G. He, M. Kolbeck, A. Garsuch, T. Bolin, *et al.*, *J. Phys. Chem. Lett.*, 2013, **4**, 3227.
38 A. Kawase, S. Shirai, Y. Yamoto, R. Arakawa and T. Takata, *Phys. Chem. Chem. Phys.*, 2014, **16**, 9344.
39 Q. Wang, J. Zheng, E. Walter, H. Pan, D. Lv, P. Zuo, H. Chen, Z. D. Deng, *et al.*, *J. Electrochem. Soc.*, 2015, **162**, A474.
40 M. Wild, L. O'Neill, T. Zhang, R. Purkayastha, G. Minton, M. Marinescu and G. J. Offer, *Energy Environ. Sci.*, 2015, **8**, 3477.

 This journal is © The Royal Society of Chemistry 2017

Open Access Article. Published on 03 July 2017. Downloaded on 9/6/2024 5:52:32 AM.
This article is licensed under a Creative Commons Attribution-NonCommercial 3.0 Unported Licence.

41 S. Han, S. Yun, O. Borodin, D. M. Seo, R. D. Sommer, V. G. Young Jr and W. A. Henderson, *J. Phys. Chem. C*, 2015, **119**, 8492.
42 D. M. Seo, O. Borodin, S. Han, Q. Ly, P. D. Boyle and W. A. Henderson, *J. Electrochem. Soc.*, 2012, **159**, A553.
43 D. M. Seo, O. Borodin, S. Han, P. D. Boyle and W. A. Henderson, *J. Electrochem. Soc.*, 2012, **159**, A1489.
44 D. M. Seo, O. Borodin, D. Balogh, M. O'Connell, Q. Ly, S. Han, S. Passerini and W. A. Henderson, *J. Electrochem. Soc.*, 2013, **160**, A1061.
45 J. W. Smith, R. K. Lam, A. T. Sheardy, O. Shih, A. M. Rizzuto, O. Borodin, S. J. Harris, D. Prendergaste and R. J. Saykally, *Phys. Chem. Chem. Phys.*, 2014, **16**, 23568.
46 O. Borodin and G. D. Smith, *J. Phys. Chem. B*, 2009, **113**, 1763.
47 M. J. Frisch, G. W. Trucks, H. B. Schlegel, G. E. Scuseria, M. A. Robb, J. R. Cheeseman, G. Scalmani, V. Barone, B. Mennucci and G. A. Petersson, *et al.*, *Gaussian 09*, Gaussian, Inc., Wallingford, CT, 2010.
48 L. E. Camacho-Forero, T. W. Smith, S. Bertolini and P. B. Balbuena, *J. Phys. Chem. C*, 2015, **119**, 26828.
49 Z. Liu, S. Bertolini, P. B. Balbuena and P. P. Mukherjee, *ACS Appl. Mater. Interfaces*, 2016, **8**, 4700.
50 J. Yeon, J. Jang, J. Han, J. Cho, K. Lee and N. Choi, *J. Electrochem. Soc.*, 2012, **159**, A1308.
51 M. Hagen, P. Schiffels, M. Hammer, S. Dorfler, J. Tubke, M. J. Hoffmann, H. Althues and S. Kaskel, *J. Electrochem. Soc.*, 2013, **160**, A1205.
52 W. Zhu, A. Paolella, C.-S. Kim, D. Liu, Z. Feng, C. Gagnon, J. Trottier, A. Vijh, A. Guerfi, A. Mauger, C. M. Julien, M. Armandd and K. Zaghib, *Sustainable Energy Fuels*, 2017, **1**, 737.
53 J. Sun, Y. Sun, M. Pasta, G. Zhou, Y. Li, W. Liu, F. Xiong and Y. Cui, *Adv. Mater.*, 2016, **28**, 9797.
54 H. Yao, K. Yan, W. Li, G. Zheng, D. Kong, Z. Seh, V. Narasimhan, Z. Liang and Y. Cui, *Energy Environ. Sci.*, 2014, **7**, 3381.